2400 *Inorg. Chem.* **1987**, *26*, 2400-2408

Contribution from the Department of Chemistry,
University of Michigan, Ann Arbor, Michigan 48109

New Members of the $[Mo_2(S)_n(S_2)_{6-n}]^{2-}$ Series. Synthesis, Structural Characterization, and Properties of the $[Mo_2S_9]^{2-}$, $[Mo_2S_7]^{2-}$, and $[Mo_2S_6]^{2-}$ Thio Anions

A. I. Hadjikyriacou and D. Coucouvanis*

Received February 18, 1987

The reactions of $(Ph_4P)_2Mo_2S_{10}/S_{12}\cdot{}^1/_2DMF$ with $NaBH_4$ and Ph_3P have been employed in the synthesis and characterization of the new thiomolybdate salts $(Ph_4P)_2Mo_2S_9$ (I), $(Ph_4P)_2Mo_2S_{6.63}$ (II), $(Ph_4P)_2Mo_2S_6$ (III), and $(Ph_4P)_2Mo_2S_7$ (IV). Both I and IV crystallize in the triclinic space group $P\bar{1}$ with two molecules per unit cell. The cell dimensions are a = 10.613 (3) Å, b = 12.352 (1) Å, c = 20.062 (2) Å, α = 99.97 (1)°, β = 103.81 (2)°, and γ = 96.64 (2)° for I and a = 10.239 (2) Å, b = 12.996 (3) Å, c = 20.438 (7) Å, α = 88.26 (2)°, β = 79.29 (2)°, and γ = 78.26 (2)° for IV. Crystals of II and III are isostructural and crystallize in the triclinic space group $P\bar{1}$ with one molecule per unit cell. The cell dimensions are a = 9.937 (2) Å, b = 10.082 (2) Å, c = 13.135 (2) Å, α = 76.14 (1)°, β = 71.68 (1)°, and γ = 70.77 (1)° for II and a = 9.932 (1) Å, b = 10.107 (2) Å, c = 13.079 (2) Å, α = 76.00 (1)°, β = 71.86 (1)°, and γ = 70.50 (1)° for III. In the structure of II the thio anions $Mo_2S_7^{2-}$ and $Mo_2S_6^{2-}$ occupy the same center of symmetry with occupancy factors 0.63 and 0.37, respectively. The asymmetric $Mo_2S_7^{2-}$ component satisfies the site symmetry requirement by assuming two equally populated centrosymmetrically disposed orientations. Intensity data for all four structures were collected with a P3/F Nicolet four-circle automated diffractometer by using the θ–2θ step scan technique. In all structures the thiomolybdate anion was refined with anisotropic temperature factors except the disordered S_4^{2-} ligand in I and the disordered sulfido/disulfido ligand in II. Full-matrix least-squares refinement, of 307 parameters on 2583 data for I, 265 parameters on 1994 data for II, 262 parameters on 1936 data for III, and 302 parameters on 3582 data for IV, gave final R values of 0.051, 0.029, 0.026, and 0.058, respectively. In I and IV the complex assumes a distorted-square-pyramidal arrangement where the terminal sulfido ligand occupies the apical position. One S_4^{2-} ligand and one MoS_4^{2-} ligand occupy the equatorial positions in I while one S_2^{2-} ligand and one MoS_4^{2-} ligand occupy the equatorial positions in IV. In I the five-coordinate molybdenum is situated 0.72 Å above the basal sulfur plane. The $Mo_2S_6^{2-}$ anion III consists of two slightly distorted tetrahedral Mo^VS_4 units that share an edge. In both asymmetric dimers I and IV the four-coordinate molybdenum atom forms shorter Mo–S bridge bonds than the five-coordinate one forms. In these complexes the charge is partially localized on the five-coordinate molybdenum atom that is slightly reduced by comparison to the four-coordinate one that appears slightly oxidized. In contrast to I and IV, the symmetric dimer III shows complete delocalization of charge. Experimental procedures for the interconversions of members of the series $[Mo_2(S)_n(S_2)_{6-n}]^{2-}$ are given in detail, and the electronic and infrared spectra for the new thiomolybdate anions are reported.

Introduction

Interest in the coordination chemistry of the binary molybdenum sulfides has intensified in recent years. This interest is due in part to the demonstrated effectiveness of "sulfided", supported molybdates as catalysts for the industrially important hydrodesulfurization reaction.[1] In these catalysts, the nature of the sites involved in either the activation of hydrogen or the cleavage of the C–S bonds is not known in any detail, and until recently, the appropriate Mo/S coordination chemistry was not available for comparative structural or reactivity studies.

The explorations in the chemistry of the binary molybdenum sulfides started with the initial reports on the synthesis and structural characterization of the $[(S_2)_2Mo(\mu\text{-}S_2)]_2^{2-}$[2a] and the $[Mo_3S_{13}]^{2-}$[2b] thio anions by Müller and co-workers. Soon thereafter, the discovery and detailed characterization of new thiomolybdates such as $[(S_4)_2MoS]^{2-}$,[3a] $[(S_2)MoS(\mu\text{-}S)]_2^{2-}$,[3b,c] $[(S_4MoS(\mu\text{-}S)]_2^{2-}$,[3a] $[(S_4)MoS(\mu\text{-}S)_2SMo(S_2)]^{2-}$,[3a,d] and $[MoS(MoS_4)_2]^{2-}$[3e] revealed the remarkable complexity of the Mo/S system.

Within the various thiomolybdate anions the molybdenum ions are found in any of three different formal oxidation states (IV, V, and VI) and are bound by S^{2-}, S_2^{2-}, or S_4^{2-} ligands in various coordination modes. A close matching of the S 3p and Mo 4d orbital energies[4] makes it possible for internal electron transfer to occur readily in some of these complexes. As a result, the sulfur atoms around the molybdenum cores in the molybdothio anions display an extraordinary intramolecular "mobility". This unique characteristic is apparent in the existence of structural isomers that can be rationalized in terms of intramolecular electron-transfer processes where S–S bonds break or form as Mo atoms are oxidized or reduced.

Among the thio anions that have been proposed to coexist in equilibria or to be possible intermediates in the formation of the $[(S_4)_2MoS]^{2-}$, $[(S_4)MoS(\mu\text{-}S)_2SMo(S_2)]^{2-}$,[3a,d] and $[MoS(MoS_4)_2]^{2-}$[3e] complexes are the $[Mo_2S_7]^{2-}$[3a,e] and $[MoS(MoS_4)(S_4)]^{2-}$[3a] anions. The former has been reported[6] to form in aqueous MoS_4^{2-} solutions at pH ~5 and to exist in the solid state,[7] while the latter, a possible precursor to $[Mo_2S_7]^{2-}$, is a hitherto unknown derivative of the well-known $(Mo{=}S)^{2+}$[3a,e] unit.

In this paper, we report in detail the synthesis and structural characterization of the previously communicated[8] $[MoS(MoS_4)(S_4)]^{2-}$ (Ia), $[Mo_2S_6]^{2-}$ (IIIa), and $[Mo_2S_7]^{2-}$ (IVa) thio anions and outline a general scheme that relates the $[Mo_2(S)_n(S_2)_{6-n}]^{2-}$ anions.

Experimental Section

Synthesis. The chemicals in this research other than solvents were used as purchased. Dimethylformamide (DMF) was distilled over CaH_2 under reduced pressure at ~30 °C unless otherwise stated. Diethyl ether was distilled after being refluxed with CaH_2 for 12 h. 2-Propanol was

---

(1) Weisser, O.; Lands, S. *Sulfide Catalysts: Their Properties and Applications*; Pergamon: London, 1973.

(2) (a) Müller, A.; Nolte, W. O.; Krebs, B. *Inorg. Chem.* **1980**, *19*, 2835. (b) Müller, A.; Bhattacharyya, R. G.; Pfefferkorn, B. *Chem. Ber.* **1979**, *112*, 778.

(3) (a) Draganjac, M.; Simhon, E.; Chan, L. T.; Kanatzidis, M.; Baenziger, N. C.; Coucouvanis, D. *Inorg. Chem.* **1982**, *21*, 3321. (b) Miller, K. F.; Bruce, A. E.; Corbin, J. L.; Wherland, S.; Stiefel, E. I. *J. Am. Chem. Soc.* **1980**, *102*, 5102. (c) Pan, W. H.; Harmer, M. A.; Halbert, T. R.; Stiefel, E. I. *J. Am. Chem. Soc.* **1984**, *106*, 459. (d) Clegg, W.; Christou, G.; Garner, C. D.; Sheldrick, G. M. *Inorg. Chem.* **1981**, *20*, 1562. (e) Pan, W. H.; Leonowicz, M. E.; Stiefel, E. I. *Inorg. Chem.* **1983**, *22*, 672.

(4) For the neutral free atoms, a compilation of Roothaan–Hartree–Fock atomic wave functions[5] shows the sulfur 3p orbitals with an energy of −0.436 94 au and the molybdenum 4d (s^1d^5) with an energy of −0.348 11 au. The localization of partial positive charge on the Mo and partial negative charge on the S is expected to bring these energies even closer together.

(5) Clementi, E.; Roetti, C. *At. Data Nucl. Data Tables* **1974**, *14*, No. 3-4.

(6) Saxena, R.; Jain, M.; Mittel, M. *Aust. J. Chem.* **1968**, *21*, 91.

(7) Mitchell, P. C. H.; Parker, D. A. *J. Chem. Soc., Dalton Trans.* **1976**, 1821.

(8) Coucouvanis, D.; Hadjikyriacou, A. I. *Inorg. Chem.* **1986**, *25*, 4317.

0020-1669/87/1326-2400$01.50/0

distilled from calcium hydride (CaH_2) before use. Dibenzyl trisulfide (BzSSSBz) was obtained as described previously.[9] Anaerobic syntheses were carried out on a Schlenk line. Elemental analyses were performed by Galbraith Analytical Laboratories, Knoxville, TN.

Physical Methods. Visible and ultraviolet electronic spectra were obtained on a Cary 219 spectrophotometer. A Debye-Scherrer camera with nickel-filtered copper radiation was utilized to obtain X-ray powder diffraction patterns. Infrared spectra were recorded on a Nicolet 5-DXB FT-IR spectrometer at a resolution of 4 cm^{-1} in KBr disks.

Preparation of Compounds. Bis(tetraphenylphosphonium) (Tetrasulfido)(tetrathiomolybdate(VI))thiomolybdate(IV), $(Ph_4P)_2[Mo(S)(MoS_4)(S_4)]$ (I). To a solution of $(Ph_4P)_2Mo_2S_{10}/S_{12}\cdot{}^1/_2DMF$[3a] (0.5 g, 0.40 mmol) in 40 mL of DMF (Aldrich 99%, used as purchased) was added 1.0 g of solid $NaBH_4$ (26.3 mmol) in air. The reaction mixture was agitated for a few minutes and then allowed to stand for 6 h. The mixture was filtered, and the filtrate was diluted with 150 mL of 2-propanol. The crude product that formed upon standing was isolated and washed with small portions of 2-propanol and diethyl ether. The brown powder so obtained was recrystallized from DMF/2-propanol. Yield: 0.15 g of thin brown needles (31%).

Anal. Calcd for $C_{48}H_{40}P_2Mo_2S_9$: C, 49.74; H, 3.45; S, 24.87. Found: C, 49.57; H, 3.67; S, 24.62. The stoichiometry of this compound also was verified by a single-crystal X-ray structure determination. The powder pattern calculated on the basis of the single-crystal data was found to be very nearly identical with that obtained for the bulk of the compound.

Bis(tetraphenylphosphonium) 0.37-[Tetrasulfidobis(μ-sulfido)dimolybdate(V)]-0.63-[trisulfido(η^2-disulfido)bis(μ-sulfido)dimolybdate(V)], $(Ph_4P)_2[Mo_2S_{6.63}]$ (II) $[(Ph_4P)_2[(Mo_2S_6)_{0.37}(Mo_2S_7)_{0.63}]]$. I (0.27 g, 0.23 mmol) was allowed to react with 0.13 g (0.49 mmol) of triphenylphosphine in 30 mL of distilled DMF. The solution was heated to 80–90 °C for 22 h, allowed to cool to ambient temperature, and filtered. To the filtrate was added 100 mL of distilled 2-propanol. When the mixture was allowed to stand, dark-brown crystals formed, were isolated, and were recrystallized from a DMF/2-propanol mixture. Yield: 0.11 g or ~43%. The stoichiometry of this compound was established by X-ray crystallography.

Bis(tetraphenylphosphonium) Tetrasulfidobis(μ-sulfido)dimolybdate(V), $(Ph_4P)_2[Mo_2S_6]$ (III). (A) From $[Mo_2S_{10}/S_{12}]^{2-}$. $(Ph_4P)_2Mo_2S_{10/12}\cdot{}^1/_2DMF$ (4.0 g, 3.21 mmol) was dissolved in 60 mL of dry DMF along with 5.0 g of Ph_3P (19.08 mmol). The reaction mixture was stirred for 4 h at 80 °C. The red solution so obtained was allowed to cool down and was then filtered. The filtrate was flooded with 2-propanol to give a red microcrystalline solid. The crude product was recrystallized from a DMF/2-propanol mixture. Yield: 2.0 g of dark-red crystals or 58%. The stoichiometry of this compound was established by single-crystal X-ray crystallography. The powder pattern calculated on the basis of the single-crystal work was found to be very nearly identical with the powder pattern of the bulk sample. Anal. Calcd for $Mo_2S_6P_2C_{48}H_{40}$: Mo, 18.08; S, 18.08; P, 5.84; C, 54.24; H, 3.77. Found: Mo, 17.94; S, 18.35; P, 5.56; C, 54.42; H, 3.86.

(B) From $[Mo_2S_8]^{2-}$. $(Ph_4P)_2Mo_2S_8$ (1.00 g, 0.89 mmol) and Ph_3P (0.48 g, 1.83 mmol) were suspended in 40 mL of freshly distilled DMF. Both reactants dissolve with stirring to give a red solution that had an orange cast. The reaction mixture was stirred for 2 h at room temperature, filtered, and flooded with diethyl ether (50 mL) to induce crystallization. Subsequent standing for 2 h afforded red crystals of $(Ph_4P)_2Mo_2S_6$. These were isolated by filtration and washed with two 20-mL portions of diethyl ether. The yield after drying in vacuo was 0.7 g (74%). Observed X-ray powder pattern *d* spacings (Å, Cu K$\bar{\alpha}$): 12.2 (m), 9.4 (w), 8.4 (w), 7.8 (vs), 7.0 (s), 6.5 (w), 5.8 (m), 5.6 (w), 5.4 (w), 4.9 (w), 4.8 (m), 4.6 (w), 4.4 (m).

Bis(tetraphenylphosphonium) Trisulfido(η^2-disulfido)bis(μ-sulfido)dimolybdate(V)–Dimethylformamide, $(Ph_4P)_2[Mo_2S_7]\cdot HCON(CH_3)_2$ (IV). An amount of $(Ph_4P)_2Mo_2S_6$ (2.00 g, 1.88 mmol) was dissolved with stirring in freshly distilled DMF (60 mL) to get a red solution with a yellow cast. Bz_2S_3 (0.53 g, 1.91 mmol) was dissolved in distilled DMF (20 mL) and was added dropwise with stirring to the thiomolybdate solution over a 2–3-min period. The reaction mixture was stirred for 12 h at room temperature. The solution turned gradually dark brown-red, which was the final color. The reaction mixture was then vacuum-filtered through a medium-porosity fritted funnel, and the filtrate was flooded with diethyl ether (100 mL) to induce crystallization. When the mixture was allowed to stand at room temperature for 2 h, brown-red microcrystalline $(Ph_4P)_2Mo_2S_7$ formed, was collected by vacuum filtration, and was washed with two 20-mL portions of diethyl ether. The yield after drying in vacuo was 1.4 g (77%). Observed X-ray powder pattern, *d* spacings (Å, Cu K$\bar{\alpha}$): 12.5 (w), 10.7 (m), 10.0 (s), 8.4 (vs), 7.7 (s), 7.0 (m), 6.5 (m), 5.9 (m), 5.0 (m), 4.8 (m), 4.6 (m), 4.4 (m), 4.2 (m). The powder pattern calculated on the basis of the single-crystal determination results, was very nearly identical with that obtained for the bulk sample above. Anal. Calcd for $(Ph_4P)_2Mo_2S_7\cdot DMF$ ($Mo_2S_7P_2C_{51}H_{47}ON$): Mo, 16.45; S, 19.19; P, 5.31; C, 52.44; H, 4.03. Found: Mo, 16.12; S, 18.76; P, 5.55; C, 52.59; H, 4.00.

Bis(tetraphenylphosphonium) Disulfidobis(η^2-disulfido)bis(μ-sulfido)dimolybdate(V), $(Ph_4P)_2[Mo_2S_8]$. (A) From $[Mo_2S_6]^{2-}$. An amount of $(Ph_4P)_2Mo_2S_6$ (2.00 g, 1.88 mmol) was dissolved with stirring in freshly distilled DMF (70 mL) to get a red solution that has a yellow cast. Bz_2S_3 (1.04 g, 3.74 mmol) was dissolved in DMF (20 mL) and was added dropwise with stirring to the thiomolybdate solution over a 2–3-min period. The reaction mixture was stirred for 12 h. As the reaction progressed the solution turned darker. Finally it attained a green cast. The reaction mixture was then filtered through a medium-porosity fritted funnel. The filtrate was flooded with diethyl ether (100 mL) to induce crystallization and allowed to stand for 2 h. The red-purple microcrystalline $(Ph_4P)_2Mo_2S_8$ was collected by vacuum filtration and washed with two 20-mL portions of diethyl ether. The yield after drying in vacuo was 1.8 g (85%). Observed X-ray powder pattern *d* spacings (Å, Cu K$\bar{\alpha}$): 12.0 (m), 11.0 (m), 9.4 (s), 8.4 (s), 7.5 (s), 6.4 (m), 4.7 (s). Anal. Calcd for $Mo_2S_8P_2C_{48}H_{40}$: Mo, 17.05; S, 22.74; P, 5.51; C, 51.15; H, 3.55. Found: Mo, 16.81; S, 23.04; P, 5.35; C, 49.99; H, 3.61.

(B) From $[Mo_2S_7]^{2-}$. $(Ph_4P)_2Mo_2S_7\cdot DMF$ (1.00 g, 0.86 mmol) was dissolved in 40 mL of freshly distilled DMF with stirring. Bz_2S_3 (0.24 g, 0.86 mmol) was dissolved in distilled DMF (10 mL) and was added to the thiomolybdate solution dropwise over a 2–3-min period. The reaction mixture was stirred for 12 h. The solution gradually turned green, which was the final color. At the end of the 12-h stirring the solution was vacuum-filtered and the filtrate was flooded with diethyl ether (60 mL). Subsequent standing for 2 h afforded 0.8 g (83%) of purple microcrystalline $(Ph_4P)_2Mo_2S_8$, which was isolated by vacuum filtration and washed with ether. The product was found to be identical with that obtained by method A. Observed X-ray powder pattern *d* spacings (Å, Cu K$\bar{\alpha}$): 12.0 (m), 11.0 (m), 9.4 (s), 8.4 (s), 7.5 (s), 6.4 (m), 4.7 (s).

Bis(tetraphenylphosphonium) Bis(μ-sulfido)((disulfido)sulfidomolybdate(V))sulfido(tetrasulfido)molybdate(V)–Hemi(dimethylformamide), $(Ph_4P)_2[Mo_2S_{10}]\cdot{}^1/_2DMF$, and Bis(tetraphenylphosphonium) Bis(μ-sulfido)bis(sulfido(tetrasulfido)molybdate(V))–Hemi(dimethylformamide), $(Ph_4P)_2[Mo_2S_{12}]\cdot{}^1/_2DMF$. (A) From $[Mo_2S_6]^{2-}$. An amount of $(Ph_4P)_2Mo_2S_6$ (1.00 g, 0.94 mmol) and Bz_2S_3 (1.57 g, 5.64 mmol) were dissolved in freshly distilled DMF (50 mL) to give an orange-red solution. The reaction mixture was stirred at room temperature for 12 h. During the initial stages of the reaction the solution was green. It finally changed to dark brown-red. The reaction mixture was then vacuum-filtered. The filtrate was flooded with diethyl ether (50 mL) to induce crystallization. After the mixture was allowed to stand for 2 h, the product that formed was isolated by vacuum filtration and washed with diethyl ether. The yield after drying in vacuo was 1.0 g (85%) of brown microcrystalline $(Ph_4P)_2Mo_2S_{10}/S_{12}\cdot{}^1/_2DMF$. Observed X-ray powder pattern *d* spacings (Å, Cu K$\bar{\alpha}$): 11.0 (vs), 10.1 (m), 9.1 (m), 8.4 (s), 7.4 (vs), 7.0 (m), 5.5 (m), 5.1 (m), 4.8 (m), 4.6 (m), 4.3 (m), 4.1 (m), 3.9–3.8 (m, diffuse), 3.4–3.35 (m, diffuse), 3.3–3.2 (m, diffuse). This compound is identical with an "authentic" sample of the previously characterized[3a] compound.

(B) From $[Mo_2S_8]^{2-}$. An amount of $(Ph_4P)_2Mo_2S_8$ (1.00 g, 0.89 mmol) and Bz_2S_3 (0.99 g, 3.55 mmol) were dissolved in freshly distilled DMF (50 mL) with stirring. The reaction mixture was stirred at room temperature for 12 h. The solution gradually changed from green to dark brown-red. The reaction mixture was then vacuum-filtered. The filtrate was flooded with diethyl ether (50 mL) to induce crystallization. After the mixture was allowed to stand for 2 h, the product was isolated by vacuum filtration and washed with diethyl ether. The yield was 0.9 g (81%) of brown microcrystalline $(Ph_4P)_2Mo_2S_{10}/S_{12}\cdot{}^1/_2DMF$. The product is identical with the one obtained above and previously.[3a]

(C) From $[Mo_2S_9]^{2-}$. An amount of $(Ph_4P)_2Mo_2S_9$ (0.79 g, 0.68 mmol) and Bz_2S_3 (0.57 g, 2.05 mmol) were dissolved in freshly distilled DMF (30 mL), and the reaction mixture was stirred for 12 h. The red reaction mixture gradually turned black-brown-red, which was the final color. At the end of the 12-h stirring, the reaction mixture was vacuum-filtered through a medium-porosity fritted funnel. The filtrate was flooded with diethyl ether (60 mL) and allowed to stand for 2 h. Then the product was isolated by vacuum filtration and washed with two 20-mL portions of diethyl ether. The yield was 0.75 g (88%) of brown microcrystalline $(Ph_4P)_2Mo_2S_{10}/S_{12}\cdot{}^1/_2DMF$.

X-ray Diffraction Measurements. Collection and Reduction of Data. Intensity data for all crystals were obtained with the use of a P3/F

---

(9) Coucouvanis, D.; Kanatzidis, M.; Simhon, E.; Baenziger, N. C. *J. Am. Chem. Soc.* **1982**, *104*, 1874.

Table I. Summary of Crystal Data, Intensity Collection, and Structure Refinement Data for $(Ph_4P)_2Mo_2S_9$ (I), $(Ph_4P)_2Mo_2S_{6.63}$ (II), $(Ph_4P)_2Mo_2S_6$ (III), and $(Ph_4P)_2Mo_2S_7$ (IV)

	I	II	III	IV
chem formula: M_r	$C_{48}H_{40}P_2Mo_2S_9$; 1159.2	$C_{48}H_{40}P_2Mo_2S_{6.63}$; 1083.2	$C_{48}H_{40}P_2Mo_2S_6$; 1063.1	$C_{51}H_{40}ONP_2Mo_2S_7$; 1168.2
a, Å	10.613 (3)	9.937 (2)	9.932 (1)	10.239 (2)
b, Å	12.352 (1)	10.082 (2)	10.107 (2)	12.996 (3)
c, Å	20.062 (2)	13.112 (2)	13.079 (2)	20.438 (7)
α, deg	99.96 (1)	76.14 (1)	76.00 (1)	88.26 (2)
β, deg	103.81 (2)	71.68 (1)	71.86 (1)	79.29 (2)
γ, deg	96.64 (2)	70.77 (1)	70.50 (1)	78.26 (2)
space group	$P\bar{1}$	$P\bar{1}$	$P\bar{1}$	$P\bar{1}$
Z; cell vol, Å^3	2; 2482	1; 1164	1; 1162	2; 2619
d_{obsd}, g/cm^3	1.53 (2)	1.54 (2)	1.49 (2)	1.52
d_{calcd}, g/cm^3	1.550	1.545	1.519	1.480
cryst dimens, mm	0.41 × 0.24 × 0.14	0.33 × 0.12 × 0.08	0.26 × 0.16 × 0.10	0.26 × 0.16 × 0.13
radiation[b]	Mo Kα	Mo Kα	Mo Kα	Mo Kα
μ, cm^{-1}	9.2	8.5	8.5	8.0
scan speed,[c] deg/min	4.0, 29.3	4.0, 29.3	3.5–29.3	3.5–29.3
std reflcns	$\bar{3}$03, 030, 004	400, 020, 002	400, 040, 002	400, 040, 002
data collcd	$\pm h,\pm k,\pm l$; $2\theta_{max}$ = 42°	$\pm h,\pm k,\pm l$; $2\theta_{max}$ = 40°	$\pm h,\pm k,\pm l$; $2\theta_{max}$ = 40°	$+h,\pm k,\pm l$; $2\theta_{max}$ = 40°
no. of unique reflcns	3048	2211	2188	4946
no. of reflcns used ($I > 3\sigma(I)$)	2583	1994	1936	3582
no. of params	307	265	262	302
R,[d] %; R_w,[d] %	5.14; 5.53	2.92; 3.18	2.55; 2.67	5.76; 5.76
largest residual, e/Å^3	0.82	0.42	0.27	1.09

[a] Density determined by flotation in a CCl_4/toluene mixture. [b] λ = 0.70926 Å. [c] Variable. [d] $R = \sum(F_o - |F_c|)/\sum F_o$; $R_w = (\sum w(F_o - |F_c|)^2/\sum wF_o{}^2)^{1/2}$.

Nicolet four-circle automated diffractometer equipped with a graphite-crystal monochromator. All data sets were measured with the θ–2θ step scan technique, and for all data sets the condition of the crystal was monitored by measuring three standard reflections periodically (every 90 reflections). Accurate parameters for all crystals were obtained from the least-squares refinement on the 2θ, φ, χ, and ω values of 25 machine-centered reflections with 2θ values between 25 and 45°.

The raw data were reduced to net intensities, estimated standard deviations were calculated on the basis of counting statistics, Lorentz–polarization corrections were applied, and equivalent reflections were averaged. The estimated standard deviation of the structure factor was taken as the larger of that derived from counting statistics and that derived from the scatter of multiple measurements.

The least-squares program used minimizes $\sum w(\Delta|F|)^2$. The weighting function used throughout the refinements of the structures gives zero weight to those reflections with $F^2 \leq 3\sigma(F^2)$ and $w = 1/\sigma^2(F)$ to all others $(\sigma^2(F^2)) = (pF^2)^2 + \sigma_1{}^2(F^2)$ (from counting statistics),[10] where p is 0.06. The procedures, atomic scattering factors, and anomalous dispersion corrections were used as described previously.[11] The refinement calculations were carried out on the University of Michigan Amdahl 800 computer using the locally adopted SHELXTL81 crystallographic package. Summary of crystal data, reflection data collection procedures, and structural refinement parameters are compiled in Table I.

(a) $(Ph_4P)_2[Mo(S)(MoS_4)(S_4)]$ (I). Crystals suitable for X-ray measurements were obtained by the slow diffusion of 2-propanol into a solution of I in DMF. A crystal was wedged in a glass capillary and a total of 11 599 reflections were collected in the full sphere of the reciprocal lattice to $2\theta_{max}$ = 42°.

(b) $(Ph_4P)_2Mo_2S_{6.63}$ (II). Crystals suitable for X-ray measurements were grown by the slow diffusion of diethyl ether into a DMF solution of $(Ph_4P)_2Mo_2S_{6.63}$. A dark red crystal was mounted at the end of a glass capillary, and intensity data were collected. A total of 4420 reflections were collected in the full sphere of the reciprocal space to 2θ = 40°.

(c) $(Ph_4P)_2Mo_2S_6$ (III). Crystals suitable for X-ray measurements were grown by the slow diffusion of 2-propanol into a DMF solution of $(Ph_4P)_2Mo_2S_6$. A red crystal was wedged in a glass capillary and intensity data were collected. A total of 4376 reflections were collected in the full sphere of the reciprocal space to 2θ = 40°.

(d) $(Ph_4P)_2Mo_2S_7$ (IV). Crystals suitable for X-ray measurements were grown by the slow diffusion of 2-propanol into a DMF solution of $(Ph_4P)_2Mo_2S_7$. A red-brown crystal was mounted at the end of a glass capillary and intensity data were collected for half of a sphere of the reciprocal space to 2θ = 40°.

During data collection no crystal decay was observed for any of the crystals, and no absorption corrections were applied to the data. For I μ = 9.2 cm^{-1}, for II μ = 8.49 cm^{-1}, for III μ = 8.51 cm^{-1}, and for IV μ = 8.0 cm^{-1}.

Solution and Refinement of Structures. (a) $(Ph_4P)_2[Mo(S)(MoS_4)(S_4)]$. The coordinates of the two Mo atoms were determined by using the direct-methods routine SOLV of the SHELXTL81 package. These positions also were verified in the Patterson map. The rest of the non-hydrogen atoms were located in subsequent difference Fourier electron density maps. Least-squares refinement with isotropic temperature factors converged to an R value of 11.8%. Anisotropic refinement of the two Mo atoms yielded a conventional R of 10.1% and revealed that S(1), S(2), and S(3) of the $S_4{}^{2-}$ ligand were disordered. Occupancy factors of 0.75 were initially assigned to S(1), S(2), and S(3), and S(1X), S(2X), and S(3X) were introduced with complementary occupancy factors of 0.25. Refinement of this model yielded an R value of 7.7%. The occupancies of the two $S_4{}^{2-}$ components converged to 0.69 and 0.31. All nondisordered atoms of the thiomolybdate and the two P atoms of the cations were refined with anisotropic thermal parameters to yield an R value of 5.9%. Finally, the position of the H atoms were calculated and included in the structure factor calculations but were not refined. The final R and R_w values were 5.14% and 5.53%, respectively.

(b) $(Ph_4P)_2Mo_2S_{6.63}$. Statistics suggested that the space group is centrosymmetric (distribution of $|E^2 - 1|$ around 0.9). The structure was solved using the direct-methods routine of the SHELX crystallographic software package. The dimer is sitting at a center of symmetry with half of the molecule comprising the asymmetric unit.

The location of the molybdenum and two of the sulfido ligands was obtained by direct methods. Subsequent difference Fourier electron density maps revealed one Ph_4P^+ cation and the terminal sulfido ligand, S(2), at the same coordination site with the disulfido ligand, S(5)–S(6). The sulfido ligand appeared with a peak height approximately twice that of a carbon, while the disulfido ligand appeared with a peak height close to that of a carbon. The positions of these disordered ligands as well as their complementary occupancies were refined. Isotropic refinement of all non-hydrogen atoms gave a conventional R value of 5.8%. All non-hydrogen atoms were refined with anisotropic temperature factors (except for the disordered ligands S(2), S(5), and S(6)) to give R = 4.3%. Finally the position of the hydrogen atoms of the cation were calculated and included in the structure factor calculation but were not refined. The occupancy of the disordered sulfido ligand S(2) converged to 0.6852 while that of the disulfido ligand S(5)–S(6) converged to the complementary occupancy of 0.3148. Final R = 2.92%; R_w = 3.18%.

(c) $(Ph_4P)_2Mo_2S_6$. Statistics suggested that the space group is centrosymmetric (distribution of $|E^2 - 1|$ around 0.9). The molecular weight calculated from the observed density and unit cell volume indicated that the dimer $Mo_2S_6{}^{2-}$ was sitting at a center of symmetry with half the dimer comprising the asymmetric unit. The coordinates of the heavy metal were obtained from the Patterson map. Subsequent difference Fourier electron density map gave the location of one bridging sulfido ligand and two terminal sulfido ligands. It also revealed one Ph_4P^+ cation sitting on a general position. Isotropic refinement of all non-hydrogen

---

(10) Grant, D. F.; Killean, R. C. G.; Lawrence, J. L. *Acta Crystallogr., Sect. B: Struct. Crystallogr. Cryst. Chem.* **1969**, *B25*, 374.

(11) Kanatzidis, M. G.; Coucouvanis, D. *Inorg. Chem.* **1984**, *23*, 403.

Table II. Electronic Spectra,[a] Mo–S Vibrational Frequencies,[b] and Calculated X-ray Powder Patterns[c] of the $(Ph_4P)_2Mo_2(S)_n(S_2)_{6-n}$ Series (n = 6, 5, 4) and of $(Ph_4P)_2Mo_2S_9$

compd	λ, nm	IR, cm^{-1}	calcd d spacings, Å
$(Ph_4P)_2Mo_2S_6$	482 (sh) 454 (ϵ = 9900) 362 (sh) 310 (ϵ = 19 300) 290 (ϵ = 26 000)	503 (m) 475 (m) 452 (w)	12.3 (m), 7.8 (vs) 7.0 (m), 5.8 (m) 4.8 (m), 4.5 (m)
$(Ph_4P)_2Mo_2S_7$	560 (ϵ = 2400) 452 (ϵ = 5200) 422 (sh) 362 (sh) 295 (sh)	504 (m) 480 (m) 454 (w)	10.7 (m), 10.0 (s) 8.5 (vs), 7.6 (m) 7.0 (m), 6.5 (m) 5.9 (m), 5.0 (m) 4.9 (m), 4.6 (m) 4.4 (m), 4.2 (m)
$(Ph_4P)_2Mo_2S_8$	574 (ϵ = 3300) 464 (ϵ = 2700) 290 (sh)	512 (sh) 453 (w)	
$(Ph_4P)_2Mo_2S_9$	422 (ϵ = 7000) 350 (sh) 298 (23 800)	(526)[d] 506 (m) 487 (m) 456 (w)	12.0 (m), 10.2 (m) 9.4 (m), 8.1 (vs) 7.6 (s), 6.9 (s) 6.2 (m), 5.0 (m) 4.9 (m), 4.7 (m) 4.3 (s)

[a] Obtained in 10^{-4}–10^{-3} DMF solutions. [b] Obtained in KBr disks on a FT-IR instrument at a resolution of 4 cm^{-1}. [c] The d spacings were calculated from single-crystal X-ray data, and only the strong and medium-intensity lines are reported. [d] Obtained from the IR spectrum of the Et_4N^+ salt.

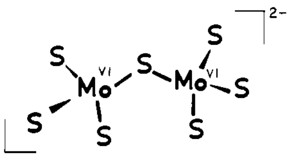

Figure 1. Possible structural isomer for the $[Mo_2S_7]^{2-}$ anion.

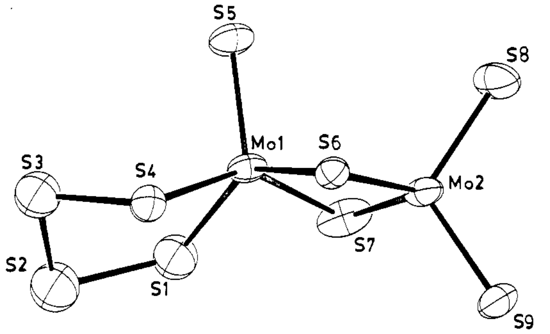

Figure 2. Structure and labeling of the $[Mo_2S_9]^{2-}$ anion (Ia). Thermal ellipsoids are drawn by ORTEP[25] and represent the 33% probability surfaces.

atoms yielded R = 6.4%. All non-hydrogen atoms were refined with anisotropic temperature factors to give R = 3.9%. The positions of the hydrogen atoms were calculated and included in the structure factor calculation but were not refined. Final R = 2.55%; R_w = 2.67%.

(d) $(Ph_4P)_2Mo_2S_7$·DMF. The location of the two molybdenum atoms were obtained from the Patterson map in $P\bar{1}$. The positions of the remaining non-hydrogen atoms were obtained by subsequent Fourier and least-squares techniques. Isotropic refinement of all non-hydrogen atoms gave R = 8.9%. The thiomolybdate anion only was allowed to refine with anisotropic temperature parameters to give R = 6.3%. Finally the positions of the hydrogen atoms were calculated and included in the structure factor calculation but were not refined. Final R = 5.76%; R_w = 5.76%.

Crystallographic Results

The final atomic positional and thermal parameters with standard deviations are compiled in Table III for $(Ph_4P)_2[Mo(S)(MoS_4)(S_4)]$, Table IV for $(Ph_4P)_2Mo_2S_6$, Table V for $(Ph_4P)_2Mo_2S_7$, and Table VI for $(Ph_4P)_2[Mo_2S_{6.63}]$. Intramolecular distances and angles are given in Tables VII and VIII.

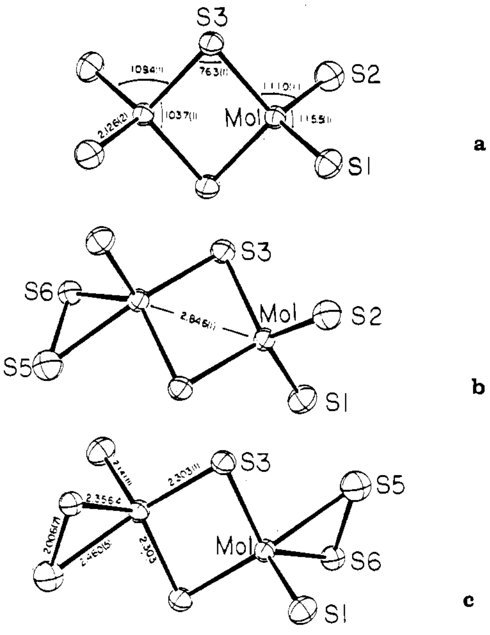

Figure 3. Structure refinement models for the anion site in $(Ph_4P)_2[Mo_2S_{6.63}]$ (II): model 1, 0.37 structure a and 0.63 structure b; model 2, 0.685 structure a and 0.315 structure c. Model 1 required two centrosymmetric orientations of structure b of equal weight. The ORTEP[25] drawings represent the 33% probability surfaces.

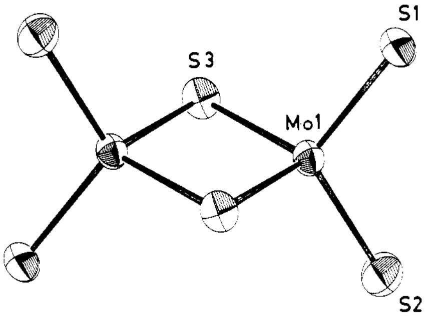

Figure 4. ORTEP[25] drawing of the $[Mo_2S_6]^{2-}$ anion (IIIa) showing the thermal ellipsoids at the 33% probability level.

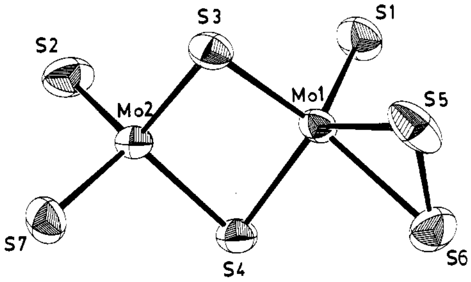

Figure 5. ORTEP[25] view of the $[Mo_2S_7]^{2-}$ anion (IVa). Atoms are represented by thermal ellipsoids at the 33% probability level.

The atom-labeling scheme is shown in Figure 2 for I, Figure 3 for II, Figure 4 for III, and Figure 5 for IV.

Results and Discussion

Synthesis and Reactivity. The $[Mo_2S_7]^{2-}$ and $[Mo_2S_9]^{2-}$ anions are proposed components in the complex equilibria that have been suggested[3a] to prevail in the reactions of MoS_4^{2-} with polysulfide ligands. The $[Mo_2S_7]^{2-}$ anion has been reported[6] to form from MoS_4^{2-} under acidic conditions and is thought to be present in solutions of MoS_4^{2-} (eq 1). There is no structural evidence to

$$2MoS_4^{2-} \rightarrow Mo_2S_7^{2-} + S^{2-} \qquad (1)$$

support the Mo(VI), $[(MoS_3)_2S]^{2-}$ structure (Figure 1), although such a structure would be analogous to the oxo analogue[12]

Table III. Atom Coordinates and Temperature Factors[a] ($Å^2 \times 10^3$) for $[(C_6H_5)_4P]_2[(S_4)Mo(S)MoS_4]$

atom	*x*	*y*	*z*	U_{eq}	atom	*x*	*y*	*z*	U_{eq}
Mo(1)	0.5552 (1)	0.8181 (1)	0.2402 (1)	0.051	C(17)	0.0353 (16)	0.8488 (10)	0.4079 (6)	0.069
Mo(2)	0.6753 (1)	1.0464 (1)	0.2911 (1)	0.053	C(18)	0.1273 (15)	0.7874 (9)	0.4386 (6)	0.063
S(1)	0.3229 (8)	0.7798 (5)	0.2190 (3)	0.083	C(19)	0.2352 (13)	0.5636 (8)	0.4988 (5)	0.045
S(2)	0.2393 (8)	0.6464 (5)	0.1316 (3)	0.101	C(20)	0.2083 (15)	0.6246 (9)	0.5569 (6)	0.062
S(3)	0.3976 (8)	0.5737 (5)	0.1252 (3)	0.089	C(21)	0.1600 (16)	0.5683 (10)	0.6032 (6)	0.072
S(1X)	0.3243 (22)	0.7221 (15)	0.2030 (9)	0.120	C(22)	0.1450 (16)	0.4550 (10)	0.5901 (6)	0.072
S(2X)	0.3300 (19)	0.5718 (10)	0.1584 (7)	0.088	C(23)	0.1750 (15)	0.3946 (9)	0.5350 (6)	0.067
S(3X)	0.3756 (17)	0.6005 (10)	0.0733 (7)	0.094	C(24)	0.2237 (14)	0.4489 (8)	0.4883 (5)	0.055
S(4)	0.5360 (4)	0.7118 (2)	0.1251 (1)	0.063	C(25)	−0.0152 (13)	0.2476 (8)	0.0074 (5)	0.043
S(5)	0.6550 (4)	0.7318 (3)	0.3125 (2)	0.071	C(26)	−0.0160 (14)	0.1735 (8)	−0.0525 (5)	0.049
S(6)	0.7198 (4)	0.9211 (2)	0.2063 (1)	0.045	C(27)	0.0599 (15)	0.2095 (9)	−0.0963 (6)	0.061
S(7)	0.4887 (5)	0.9664 (3)	0.3082 (2)	0.091	C(28)	0.1303 (16)	0.3147 (10)	−0.0813 (6)	0.076
S(8)	0.8343 (5)	1.0788 (3)	0.3844 (1)	0.084	C(29)	0.1275 (17)	0.3888 (11)	−0.0227 (7)	0.085
S(9)	0.6431 (5)	1.1935 (2)	0.2493 (2)	0.077	C(30)	0.0514 (16)	0.3546 (10)	0.0233 (6)	0.073
P(1)	0.2984 (4)	0.6372 (2)	0.4390 (1)	0.041	C(31)	−0.1725 (15)	0.3142 (8)	0.1062 (5)	0.043
P(2)	−0.1052 (4)	0.2030 (2)	0.0658 (1)	0.042	C(32)	−0.3013 (17)	0.3265 (10)	0.0762 (6)	0.070
C(1)	0.4457 (13)	0.7329 (7)	0.4850 (4)	0.038	C(33)	−0.3571 (18)	0.4114 (12)	0.1092 (8)	0.105
C(2)	0.5171 (14)	0.7246 (8)	0.5511 (5)	0.047	C(34)	−0.2864 (18)	0.4787 (10)	0.1699 (7)	0.072
C(3)	0.6309 (15)	0.8000 (9)	0.5841 (6)	0.063	C(35)	−0.1598 (17)	0.4724 (9)	0.1989 (6)	0.065
C(4)	0.6731 (16)	0.8805 (10)	0.5513 (6)	0.073	C(36)	−0.1031 (15)	0.3860 (10)	0.1670 (6)	0.066
C(5)	0.6051 (15)	0.8871 (10)	0.4860 (6)	0.065	C(37)	0.0088 (16)	0.1578 (8)	0.1345 (5)	0.040
C(6)	0.4895 (15)	0.8146 (9)	0.4524 (5)	0.054	C(38)	−0.0415 (14)	0.1382 (8)	0.1924 (5)	0.049
C(7)	0.3341 (19)	0.5380 (8)	0.3725 (5)	0.038	C(39)	0.0415 (18)	0.0915 (9)	0.2446 (5)	0.055
C(8)	0.2299 (15)	0.4573 (9)	0.3275 (5)	0.058	C(40)	0.1602 (19)	0.0698 (9)	0.2357 (6)	0.061
C(9)	0.2597 (21)	0.3790 (9)	0.2764 (6)	0.065	C(41)	0.2073 (15)	0.0916 (9)	0.1803 (5)	0.056
C(10)	0.3858 (21)	0.3810 (9)	0.2695 (6)	0.061	C(42)	0.1283 (17)	0.1339 (9)	0.1290 (5)	0.049
C(11)	0.4842 (15)	0.4586 (9)	0.3141 (6)	0.061	C(43)	−0.2290 (13)	0.0903 (7)	0.0181 (4)	0.034
C(12)	0.4578 (19)	0.5380 (8)	0.3659 (5)	0.046	C(44)	−0.2502 (13)	−0.0090 (8)	0.0418 (5)	0.042
C(13)	0.1806 (12)	0.7127 (7)	0.3980 (5)	0.038	C(45)	−0.3457 (14)	−0.0964 (8)	0.0036 (5)	0.048
C(14)	0.1416 (15)	0.6995 (9)	0.3265 (6)	0.062	C(46)	−0.4283 (14)	−0.0865 (8)	−0.0592 (5)	0.053
C(15)	0.0435 (17)	0.7638 (10)	0.2990 (6)	0.075	C(47)	−0.4102 (14)	0.0110 (8)	−0.0828 (5)	0.050
C(16)	−0.0034 (15)	0.8367 (9)	0.3377 (6)	0.063	C(48)	−0.3144 (13)	0.0990 (8)	−0.0467 (5)	0.045

[a] Equivalent isotropic *U* defined as one-third of the trace of the orthogonalized $\mathbf{U}_{ij}$ tensor.

Table IV. Atom Coordinates and Temperature Factors[a] ($Å^2 \times 10^3$) for $[(C_6H_5)_4P][Mo_2S_6]$

atom	*x*	*y*	*z*	U_{eq}	atom	*x*	*y*	*z*	U_{eq}
Mo(1)	0.3513 (1)	0.0603 (1)	0.0568 (1)	0.038	C(11)	−0.2140 (6)	0.1691 (5)	0.1887 (4)	0.063
S(1)	0.2926 (1)	0.1277 (1)	0.2132 (1)	0.052	C(12)	−0.1509 (5)	0.2400 (5)	0.2314 (4)	0.055
S(2)	0.1644 (1)	0.0959 (2)	−0.0057 (1)	0.071	C(13)	0.0092 (5)	0.5050 (5)	0.2265 (4)	0.041
S(3)	0.5141 (1)	0.1750 (1)	−0.0664 (1)	0.047	C(14)	0.0662 (6)	0.5930 (6)	0.2567 (4)	0.073
P(1)	−0.1470 (1)	0.4551 (1)	0.3219 (1)	0.039	C(15)	0.1831 (7)	0.6380 (7)	0.1849 (5)	0.089
C(1)	−0.2766 (5)	0.6157 (4)	0.3665 (4)	0.040	C(16)	0.2438 (6)	0.5944 (6)	0.0856 (4)	0.067
C(2)	−0.3425 (5)	0.6296 (5)	0.4744 (4)	0.050	C(17)	0.1885 (6)	0.5051 (6)	0.0561 (4)	0.060
C(3)	−0.4441 (6)	0.7574 (6)	0.5013 (4)	0.060	C(18)	0.0691 (5)	0.4607 (5)	0.1271 (4)	0.049
C(4)	−0.4790 (5)	0.8675 (5)	0.4199 (5)	0.063	C(19)	−0.0941 (5)	0.3285 (4)	0.4349 (3)	0.042
C(5)	−0.4122 (6)	0.8543 (5)	0.3137 (5)	0.063	C(20)	−0.2020 (6)	0.2723 (5)	0.5118 (4)	0.063
C(6)	−0.3109 (5)	0.7286 (5)	0.2861 (4)	0.052	C(21)	−0.1669 (7)	0.1698 (6)	0.5972 (4)	0.075
C(7)	−0.2308 (5)	0.3727 (5)	0.2609 (3)	0.040	C(22)	−0.0245 (8)	0.1217 (5)	0.6057 (5)	0.078
C(8)	−0.3719 (5)	0.4351 (5)	0.2470 (4)	0.051	C(23)	0.0832 (6)	0.1760 (6)	0.5311 (5)	0.067
C(9)	−0.4333 (6)	0.3603 (7)	0.2051 (4)	0.067	C(24)	0.0490 (5)	0.2805 (5)	0.4443 (4)	0.050
C(10)	−0.3542 (7)	0.2294 (6)	0.1770 (4)	0.067					

[a] Equivalent isotropic *U* as defined in footnote *a* of Table III.

$[(MoO_3)_2O]^{2-}$ and consistent with the proposed[7] coordination characteristics of the $[Mo_2S_7]^{2-}$ ligand in the $[Fe(Salen)]_2(Mo_2S_7)$ complex.

The $[MoS(MoS_4)(S_4)]^{2-}$ anion could be considered as the conproportionation product of the known $[(S_4)_2MoS]^{2-}$[3a] and $[MoS(MoS_4)_2]^{2-}$[3e] complexes (eq 2) and would contain the

$$[(S_4)_2MoS]^{2-} + [MoS(MoS_4)_2]^{2-} \rightarrow 2[MoS(MoS_4)(S_4)]^{2-} \quad (2)$$

$(Mo{=}S)^{2+}$ unit coordinated by the S_4^{2-} and MoS_4^{2-} ligands. The $[MoS(MoS_4)(S_4)]^{2-}$ complex was sought initially with the anticipation that this compound also could serve as a source for the $[Mo_2S_7]^{2-}$ anion by the procedure shown in Scheme I.

The synthesis of $[Ph_4P]_2[MoS(MoS_4)(S_4)]$ can be carried out by the reduction of $[Ph_4P]_2[(S_4)MoS(\mu\text{-}S)_2SMo(S_2)]$[3a] with NaBH$_4$ in DMF, and the product is obtained in crystalline form in ~30% yield. A possible mechanism for this reaction is shown in Scheme II where the generation of the MoS_4^{2-} ligand in the

Scheme I

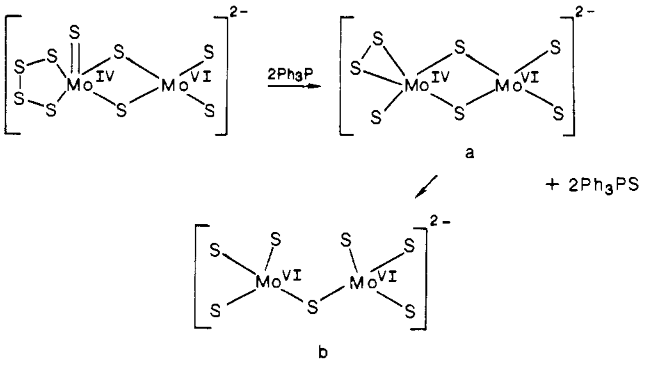

---

(12) Day, V. W.; Fredrich, M. F.; Klemperer, W. G.; Shum, W. *J. Am. Chem. Soc.* **1977**, *99*, 6146.

Table V. Atom Coordinates and Temperature Factors[a] ($Å^2 \times 10^3$) for $[(C_6H_5)_4P]_2[(S_2)Mo(S)MoS_4]$

atom	x	y	z	U_{eq}	atom	x	y	z	U_{eq}
Mo(1)	0.4822 (1)	0.2942 (1)	0.2863 (1)	0.051	C(22)	1.1912 (15)	0.6372 (12)	0.5461 (8)	0.095
Mo(2)	0.6032 (1)	0.0963 (1)	0.2240 (1)	0.050	C(23)	1.1378 (14)	0.7418 (11)	0.5628 (7)	0.081
S(1)	0.5329 (4)	0.4133 (3)	0.2206 (2)	0.078	C(24)	1.0434 (13)	0.8002 (10)	0.5244 (6)	0.066
S(2)	0.7329 (4)	0.0938 (3)	0.1293 (2)	0.081	C(25)	0.4024 (11)	0.6963 (8)	0.0535 (5)	0.047
S(3)	0.3879 (3)	0.1889 (3)	0.2256 (2)	0.066	C(26)	0.4921 (12)	0.6163 (9)	0.0788 (6)	0.055
S(4)	0.6812 (3)	0.1809 (2)	0.3009 (2)	0.060	C(27)	0.6073 (13)	0.5623 (10)	0.0375 (6)	0.064
S(5)	0.2717 (4)	0.3526 (3)	0.3603 (2)	0.090	C(28)	0.6336 (14)	0.5864 (10)	−0.0278 (7)	0.073
S(6)	0.4498 (5)	0.3570 (3)	0.3988 (2)	0.091	C(29)	0.5462 (14)	0.6642 (1)	−0.0539 (6)	0.075
S(7)	0.5937 (4)	−0.0609 (3)	0.2614 (2)	0.076	C(30)	0.4289 (13)	0.7210 (10)	−0.0152 (6)	0.070
P(1)	0.8965 (3)	0.8261 (2)	0.4243 (1)	0.047	C(31)	0.1032 (12)	0.7417 (9)	0.0917 (6)	0.054
P(2)	0.2580 (3)	0.7710 (2)	0.1056 (2)	0.052	C(32)	0.0967 (13)	0.6820 (10)	0.0371 (6)	0.071
C(1)	0.8159 (11)	0.7377 (8)	0.3880 (5)	0.047	C(33)	−0.0326 (16)	0.6671 (11)	0.0300 (7)	0.088
C(2)	0.7049 (13)	0.7028 (10)	0.4254 (6)	0.063	C(34)	−0.1450 (16)	0.7059 (12)	0.0724 (8)	0.092
C(3)	0.6462 (13)	0.6299 (10)	0.3986 (6)	0.066	C(35)	−0.1410 (15)	0.7670 (11)	0.1261 (7)	0.091
C(4)	0.6954 (14)	0.5943 (10)	0.3361 (7)	0.071	C(36)	−0.0131 (14)	0.7819 (10)	0.1348 (6)	0.071
C(5)	0.8035 (15)	0.6230 (11)	0.2991 (7)	0.083	C(37)	0.2580 (11)	0.9080 (8)	0.0892 (5)	0.049
C(6)	0.8671 (14)	0.6969 (10)	0.3246 (7)	0.075	C(38)	0.3748 (12)	0.9445 (9)	0.0872 (6)	0.057
C(7)	0.9867 (11)	0.8957 (8)	0.3606 (5)	0.044	C(39)	0.3747 (14)	1.0520 (10)	0.0751 (6)	0.071
C(8)	0.9258 (12)	0.9338 (9)	0.3065 (6)	0.053	C(40)	0.2588 (15)	1.1179 (11)	0.0649 (7)	0.081
C(9)	0.9925 (12)	0.9969 (9)	0.2594 (6)	0.057	C(41)	0.1404 (15)	1.0826 (12)	0.0662 (7)	0.089
C(10)	1.1125 (13)	1.0193 (9)	0.2652 (6)	0.062	C(42)	0.1390 (13)	0.9732 (10)	0.0782 (6)	0.062
C(11)	1.1735 (14)	0.9781 (10)	0.3184 (7)	0.076	C(43)	0.2753 (11)	0.7364 (9)	0.1896 (5)	0.050
C(12)	1.1093 (13)	0.9173 (9)	0.3673 (6)	0.061	C(44)	0.3565 (13)	0.7787 (10)	0.2220 (6)	0.067
C(13)	0.7706 (10)	0.9181 (8)	0.4768 (5)	0.041	C(45)	0.3838 (14)	0.7371 (11)	0.2840 (7)	0.079
C(14)	0.7156 (11)	0.8875 (9)	0.5395 (6)	0.051	C(46)	0.3271 (13)	0.6535 (10)	0.3108 (6)	0.070
C(15)	0.6176 (12)	0.9584 (9)	0.5790 (6)	0.056	C(47)	0.2479 (14)	0.6113 (10)	0.2792 (7)	0.074
C(16)	0.5757 (12)	1.0605 (9)	0.5578 (6)	0.058	C(48)	0.2189 (12)	0.6511 (9)	0.2163 (6)	0.063
C(17)	0.6327 (12)	1.0914 (9)	0.4963 (6)	0.060	N(1)	−0.0143 (16)	0.3578 (12)	0.2004 (8)	0.128
C(18)	0.7281 (11)	1.0202 (8)	0.4554 (5)	0.048	C(C1)	0.0958 (21)	0.4105 (16)	0.1894 (11)	0.134
C(19)	1.0087 (11)	0.7504 (9)	0.4740 (5)	0.049	O(1)	0.0876 (21)	0.4565 (16)	0.1366 (11)	0.252
C(20)	1.0611 (13)	0.6452 (10)	0.4590 (6)	0.071	C(C3)	−0.0134 (23)	0.3144 (18)	0.2694 (12)	0.180
C(21)	1.1564 (15)	0.5884 (12)	0.4967 (8)	0.094	C(C4)	−0.1141 (24)	0.3743 (18)	0.1571 (12)	0.181

[a] Equivalent isotropic U as defined in footnote a of Table III.

Table VI. Atom Coordinates and Temperature Factors[a] ($Å^2 \times 10^3$) for $(Ph_4P)_2Mo_2S_{6.63}$

atom	x	y	z	U_{eq}	atom	x	y	z	U_{eq}
Mo(1)	0.8515 (1)	0.0554 (1)	0.5582 (1)	0.036	C(10)	0.5246 (9)	0.8787 (6)	−0.1059 (5)	0.073
S(1)	0.7976 (2)	0.1266 (2)	0.7111 (1)	0.056	C(11)	0.6675 (7)	0.8304 (6)	−0.0974 (5)	0.070
S(2)	0.6692 (3)	0.0817 (3)	0.4962 (2)	0.063	C(12)	0.7020 (6)	0.7282 (5)	−0.0123 (4)	0.057
S(3)	0.9938 (1)	−0.1772 (1)	0.5691 (1)	0.045	C(13)	0.4894 (5)	0.4949 (5)	0.2722 (4)	0.039
S(5)	0.6423 (5)	−0.0332 (5)	0.5726 (4)	0.066	C(14)	0.4291 (6)	0.5388 (5)	0.3723 (4)	0.048
S(6)	0.6430 (5)	0.1607 (6)	0.4878 (3)	0.043	C(15)	0.3097 (6)	0.4950 (6)	0.4422 (4)	0.056
P(1)	0.3542 (1)	0.4552 (1)	0.8232 (1)	0.037	C(16)	0.2520 (6)	0.4084 (6)	0.4122 (5)	0.061
C(1)	0.7301 (5)	0.6271 (5)	0.2379 (4)	0.039	C(17)	0.3116 (7)	0.3647 (7)	0.3123 (5)	0.082
C(2)	0.6525 (6)	0.7593 (5)	0.2672 (4)	0.053	C(18)	0.4302 (6)	0.4075 (6)	0.2414 (4)	0.068
C(3)	0.7156 (7)	0.8293 (6)	0.3107 (4)	0.063	C(19)	0.7750 (5)	0.3847 (5)	0.1317 (4)	0.040
C(4)	0.8548 (7)	0.7670 (7)	0.3231 (4)	0.069	C(20)	0.8075 (6)	0.2706 (5)	0.2124 (4)	0.052
C(5)	0.9330 (6)	0.6351 (7)	0.2951 (4)	0.065	C(21)	0.9098 (6)	0.1457 (6)	0.1846 (5)	0.061
C(6)	0.8705 (5)	0.5619 (5)	0.2525 (4)	0.048	C(22)	0.9784 (6)	0.1334 (6)	0.0784 (6)	0.061
C(7)	0.5937 (5)	0.6726 (5)	0.0648 (4)	0.040	C(23)	0.9455 (6)	0.2437 (7)	−0.0025 (5)	0.061
C(8)	0.4494 (5)	0.7216 (5)	0.0560 (4)	0.048	C(24)	0.8429 (5)	0.3714 (5)	0.0232 (4)	0.048
C(9)	0.4164 (6)	0.8259 (6)	−0.0307 (5)	0.063					

[a] Equivalent isotropic U as defined in footnote a of Table III.

$[MoS(MoS_4)(S_4)]^{2-}$ anion (Ia) occurs as a result of internal electron transfer following the reduction of the $[(S_4)MoS(\mu\text{-}S)_2SMo(S_2)]^{2-}$ complex.

The reaction of I with 2 equiv of Ph_3P in DMF, proceeds essentially as indicated in Scheme I to give the a isomer of $[Mo_2S_7]^{2-}$ (IVa); however, the product contains a significant amount of the $[Mo_2S_6]^{2-}$ anion (IIIa). The latter apparently forms as a result of rapid further reaction of Ph_3P with the $[Mo_2S_7]^{2-}$ anion. The two anions cocrystallize and were found to occupy the same site in the crystal (vide infra). Pure crystalline $[Ph_4P]_2[Mo_2S_6]$ can be obtained in good yield, as the final product of the reaction of $[Ph_4P]_2[(S_4)MoS(\mu\text{-}S)_2SMo(S_2)]$ with 6 equiv of Ph_3P in DMF solution. The synthesis of pure $[Ph_4P]_2[Mo_2S_7]$ can be obtained in good yield by the addition of S to $[Ph_4P]_2[Mo_2S_6]$ using BzSSSBz[9] as a sulfur transfer reagent. The general applicability of the BzSSSBz reagent for the synthesis of pure $[Mo_2(S)_n(S_2)_{6-n}]^{2-}$ thio anions in stoichiometric reactions is aptly illustrated in the synthesis of the $[Ph_4P]^+$ salts of the $[Mo_2S_7]^{2-}$, $[Mo_2S_8]^{2-}$, and $[Mo_2S_{10}/S_{12}]^{2-}$ anions from either $[Ph_4P]_2[Mo_2S_6]$ or, where appropriate, from higher sulfur content $[Mo_2(S)_n(S_2)_{6-n}]^{2-}$ anions (see Experimental Section). Interconversions between these thio anions by the removal of sulfur with Ph_3P also can be accomplished readily.

Scheme II

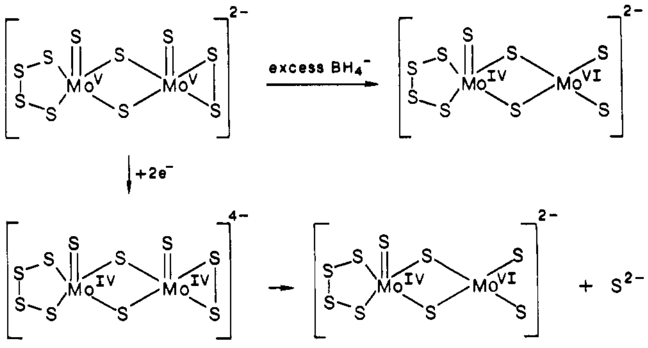

Table VII. Selected Interatomic Distances (Å) and Angles (deg) in the $[(S_4)Mo(S)(MoS_4)]^{2-}$ Anion (Figure 2)

	Distances		
Mo(1)–Mo(2)	2.859 (1)		
Mo(1)–S(1)	2.376 (9)	Mo(1)–S(X1)	2.47 (2)
Mo(1)–S(4)	2.399 (3)		
Mo(1)–S(6)	2.342 (4)		
Mo(1)–S(7)	2.368 (4)		
mean	2.37 (4, 1)		
Mo(1)–S(5)	2.105 (3)		
Mo(2)–S(6)	2.271 (3)		
Mo(2)–S(7)	2.237 (5)		
Mo(2)–S(8)	2.142 (4)		
Mo(2)–S(9)	2.157 (3)		
mean	2.20 (4, 3)		
S(1)–S(2)	2.120 (8)	S(1)–S(7)	2.783 (8)
S(2)–S(3)	2.015 (11)	S(1)–S(4)	3.360 (9)
S(3)–S(4)	2.119 (8)	S(1)–S(3)	3.189 (10)
		S(4)–S(6)	3.000 (4)
S(1X)–S(2X)	1.93 (2)	S(1X)–S(4)	3.03 (2)
S(2X)–S(3X)	1.96 (2)	S(1X)–S(3X)	2.97 (2)
S(3X)–S(4)	2.00 (2)	S(2X)–S(4)	2.91 (2)
		S(1X)–S(7)	3.38 (2)
	Angles		
S(4)–Mo(1)–S(1)	89.5 (2)	S(4)–Mo(1)–S(1X)	76.9 (4)
S(1)–Mo(1)–S(5)	113.2 (2)	S(1X)–Mo(1)–S(5)	105.3 (4)
S(4)–Mo(1)–S(5)	107.0 (1)		
S(5)–Mo(1)–S(6)	105.4 (2)		
S(5)–Mo(1)–S(7)	105.6 (1)		
S(1)–Mo(1)–S(7)	71.8 (2)	S(1X)–Mo(1)–S(7)	88.5 (5)
S(1)–Mo(1)–S(6)	141.4 (2)	S(1X)–Mo(1)–S(6)	145.6 (4)
S(4)–Mo(1)–S(6)	78.5 (2)		
S(4)–Mo(1)–S(7)	146.8 (1)		
S(6)–Mo(1)–S(7)	99.0 (1)		
S(6)–Mo(2)–S(7)	105.2 (1)		
S(9)–Mo(2)–S(8)	112.9 (1)		
Mo(1)–S(6)–Mo(2)	76.6 (1)		
Mo(1)–S(7)–Mo(2)	76.7 (1)		

Spectroscopic Properties. The electronic spectra and the Mo–S vibrations of the complexes are tabulated in Table II. A feature in the electronic spectra that appears to be associated with the $Mo^V–S_2$ fragment is a low-energy electronic absorption that occurs above 550 nm and most likely is due to a $Mo–S_2$ charge transfer. This absorption that occurs at 560 nm and 574 nm in $[Mo_2S_7]^{2-}$ and $[Mo_2S_8]^{2-}$, respectively, is not present in the spectra of either $[Mo_2S_6]^{2-}$ or $[Mo_2S_9]^{2-}$. However it is observed in the spectrum of $[Mo_2(S_2)_6]^{2-}$ that shows two bands at 769 and 625 nm. Similar low-energy absorption bands also are observed in the spectra of the $[(S_4)MoS(\mu\text{-}S)_2SMo(S_2)]^{2-}$ and $MoO(S_2)(Et_2NCS_2)_2$ complexes. In the latter[13] an absorption at 580 nm (ϵ = 1300) has been assigned previously[14] to a $\pi^*_v(\eta^2\text{-}S_2^{2-}) \rightarrow d(Mo)$ charge-transfer process.

The electronic spectrum of $[(S_4)MoS(MoS_4)]^{2-}$ (Ia) shows a strong electronic absorption band at 422 nm and indicates the presence of perturbed MoS_4^{2-}. The $S \rightarrow Mo(\pi(t_1) \rightarrow d(e))$ transition[15] in MoS_4^{2-} appears at 470 nm, and in the Fe-Mo-S complexes derived from MoS_4^{2-}, the same transition appears at 460 ± 40 nm.[16]

The infrared spectra of the complexes (Table II) show multiple absorptions between 530 and 450 cm^{-1} that can be assigned to the $Mo{=}S_t$ and $Mo{-}S_b$ stretching vibrations. In the spectra of the $[Mo_2(S)_n(S_2)_{6-n}]^{2-}$ anions the high-frequency bands at 503, 504, and 512 cm^{-1} for n = 6, 5, and 4, respectively, are assigned to the $Mo{=}S_t$ vibrations. The bands below 500 cm^{-1} are assigned to $Mo{-}S_b$ vibrations. Similar assignments have been made previously for the Mo–S vibrations in the $[Mo_2(S)_4(S_2)_2]^{2-}$ and $[(MoS_4)_2MoS]^{2-}$ complexes.[3b,c,e] In the $[(S_4)_n(MoS_4)_{2-n}Mo^{IV}S]^{2-}$ complexes the $Mo{=}S_t$ vibrations are found at 527, 526, and 525 cm^{-1} for n = 0,[3e] 1, and 2,[3a] respectively. This similarity is somewhat surprising in view of an apparently systematic variation in the $Mo(IV){=}S_t$ bond lengths (vide infra). The latter are found at 2.086 (4),[3e] 2.105 (3), and 2.128 (1) Å[3a] for n = 0, 1, and 2 respectively. It is possible that the expected increase in the vibrational frequency of the $Mo{=}S_t$ bond is offset by kinematic effects. The latter are expected to become increasingly important as the S_4^{2-} ligands are replaced by the MoS_4^{2-} ligands.

Table VIII. Selected Interatomic Distances (Å) and Angles (deg) in the $[Mo_2S_{6.63}]^{2-}$, $[Mo_2S_6]^{2-}$, $[Mo_2S_7]^{2-}$, and $[Mo_2S_8]^{2-}$ Anions (Figures 3–5)

Distances

	$[Mo_2S_{6.63}]^{2-}$	$[Mo_2S_6]^{2-}$	$[Mo_2S_7]^{2-}$	$[Mo_2S_8]^{2-}$ [a]
Mo–Mo	2.846 (1)	2.856 (1)	2.848 (2)	2.821 (1)
Mo(1)–S(1)	2.141 (1)	2.157 (1)	2.103 (3)	2.128 (1)
Mo(1)–S(2)	2.126 (2)	2.145 (1)		
Mo(1)–S(3)	2.303 (1)	2.298 (1)	2.326 (4)	2.306 (1)
Mo(1)–S(3)′	2.303 (1)	2.301 (1)		
Mo(1)–S(4)			2.319 (3)	2.308 (2)
Mo(1)–S(5)	2.459 (5)		2.399 (4)	2.403 (1)
Mo(1)–S(6)	2.356 (4)		2.408 (4)	2.375 (2)
Mo(2)–S(2)			2.141 (4)	2.108 (1)
Mo(2)–S(3)			2.282 (3)	2.314 (1)
Mo(2)–S(4)			2.285 (3)	2.313 (1)
Mo(2)–S(7)			2.174 (3)	
S(1)–S(2)	3.609 (3)	3.592 (2)		
S(1)–S(3)	3.629 (2)	3.645 (2)		
S(1)–S(3)′	3.614 (3)	3.654 (2)		
S(2)–S(3)	3.651 (3)	3.628 (2)		
S(2)–S(3)′	3.578 (3)	3.657 (2)		
S(3)–S(7)			3.625 (5)	
S(2)–S(7)			3.581 (5)	
S(4)–S(7)			3.590 (5)	
S(3)–S(3)′	3.622 (2)	3.605 (2)		
S(3)–S(4)			3.592 (4)	
S(5)–S(6)	2.006 (7)		2.123 (6)	2.051 (2)

Angles

	$[Mo_2S_{6.63}]^{2-}$	$[Mo_2S_6]^{2-}$	$[Mo_2S_7]^{2-}$
Mo–S(3)–Mo	76.3 (1)	76.8 (1)	76.3 (1)
Mo–S(4)–Mo			76.4 (1)
S(1)–Mo(1)–S(2)	115.5 (1)	113.3 (1)	
S(1)–Mo(1)–S(3)	109.4 (1)	109.8 (1)	105.3 (1)
S(1)–Mo(1)–S(3)′	108.8 (1)	110.1 (1)	
S(1)–Mo(1)–S(4)			108.2 (1)
S(1)–Mo(1)–S(5)	103.4 (1)		111.9 (1)
S(1)–Mo(1)–S(6)	106.7 (1)		109.0 (1)
S(2)–Mo(1)–S(3)	111.0 (1)	109.4 (1)	
S(2)–Mo(1)–S(3)′	107.7 (1)	110.6 (1)	
S(3)–Mo(1)–S(3)′	103.7 (1)	103.2 (1)	
S(3)–Mo(1)–S(4)			101.3 (1)
S(3)–Mo(1)–S(5)			92.6 (2)
S(3)–Mo(1)–S(6)			138.0 (1)
S(4)–Mo(1)–S(5)			132.0 (1)
S(4)–Mo(1)–S(6)			90.3 (1)
S(5)–Mo(1)–S(6)	49.2 (2)		52.4 (2)
S(3)–Mo(2)–S(2)			114.0 (1)
S(3)–Mo(2)–S(4)			103.7 (1)
S(2)–Mo(2)–S(4)			110.3 (1)
S(2)–Mo(2)–S(7)			112.2 (2)
S(3)–Mo(2)–S(7)			108.9 (1)
S(4)–Mo(2)–S(7)			107.2 (1)

[a] From ref 3c.

Structures. $[Ph_4P]_2[(S_4)Mo^{IV}S(MoS_4)]^{2-}$. The structure of the anion in I can be described as a square-pyramidal $[(L)(L')Mo^{IV}S]^{2-}$ complex where the $[Mo^{IV}S]^{2+}$ unit is coordinated by the S_4^{2-} and $[MoS_4]^{2-}$ ligands. This type of structure is rather common for the $[Mo^{IV}S]^{2+}$ chromophore and I is a mixed-ligand

---

(13) McDonald, J. W.; Newton, W. E. *Inorg. Chim. Acta* **1980**, *44*, L81.

(14) Müller, A.; Jaegermann, W.; Enemark, J. H. *Coord. Chem. Rev.* **1982**, *46*, 273.

(15) (a) Stiefel, E. I. *Progr. Inorg. Chem.* **1977**, *22*, 1 and references therein. (b) Diemann, E.; Müller, A. *Coord. Chem. Rev.* **1973**, *10*, 79.

(16) Coucouvanis, D. *Acc. Chem. Res.* **1981**, *14*, 201.

analogue of the well-characterized $[(S_4)_2Mo^{IV}S]^{2-}$ and $[(MoS_4)_2Mo^{IV}S]^{2-}$ anions. As found in the latter two complexes the Mo(IV) center in I also is elevated above the basal, S(1)S(4)S(6)S(7), plane by 0.72 Å. The interatomic distances and angles in I (Table VI) are similar to corresponding structural features in $[(S_4)_2Mo^{IV}S]^{2-}$[3a] and $[(MoS_4)_2Mo^{IV}S]^{2-}$.[3e] An examination of the $[Mo^{IV}S]^{2+}$ units in the three related anions shows that the Mo–S_t bond decreases in length as the $[MoS_4]^{2-}$ ligands replace the S_4^{2-} ligands in the coordination sphere of the $[(S_4)_n(MoS_4)_{2-n}Mo^{IV}S]^{2-}$ complexes. The Mo–S_t bonds are 2.086 (4), 2.105 (3), and 2.128 (1) Å for $n = 0$, 1, and 2, respectively. The delocalization of charge toward the $[MoS_4]^{2-}$ ligands (and away from the $[Mo^{IV}S]^{2+}$ centers) suggested by this systematic variation also is apparent in the mean values of the Mo–S bonds in the coordinated $[MoS_4]^{2-}$ ligands. These values at 2.202 (5) and 2.191 (4) Å in I and $[(MoS_4)_2Mo^{IV}S]^{2-}$, respectively, are longer than the Mo–S bond in $(Et_4N)_2MoS_4$ (2.177 (6) Å).[17] They are similar however to the Mo–S bonds observed for the coordinated $[MoS_4]^{2-}$ ligands in the $[(PhS)_2FeS_2MoS_2]^{2-}$ anion[18] (2.205 (2) Å) the $[(S_5)_2FeS_2MoS_2]^{2-}$ anion[18,19] (2.204 (6) Å), and the $[Cl_2FeS_2MoS_2FeCl_2]^{2-}$ anion[20] (2.206 (2) Å). The lengthening of the Mo–S bonds in the Fe/MoS_4 complexes has been attributed previously to a shift of electron density from the Fe(II) ions to the empty d_{z^2} orbitals of the Mo(VI) ions.[16,18–20]

The participation of the Mo(IV) center in d_π–p_π bonding with the S donor atoms of the S_4^{2-} ligand in I accounts for the alternation in the S–S bond lengths in the S_4^{2-} ligand. This alternation is a common feature in all of the Mo–S_4 complexes that have been characterized structurally and has been discussed previously.[21] The S_4^{2-} ligand in I has the "half-envelope" configuration. The same configuration is found for this ligand in the $[(S_4)_2Mo^{IV}S]^{2-}$ anion.[3a]

$[Ph_4P]_2[Mo_2S_{6.63}]$, $[Ph_4P]_2[Mo_2S_6]$, and $[Ph_4P]_2[Mo_2S_7]$. The new thio anions $[Mo_2S_6]^{2-}$ and $[Mo_2S_7]^{2-}$ occupy the same center of symmetry in the structure of $[Ph_4P]_2[Mo_2S_{6.63}]$. The centrosymmetric $[Mo_2S_6]^{2-}$ anion is found at the site with a 0.37 occupancy factor. The asymmetric $[Mo_2S_7]^{2-}$ component is present with an occupancy factor of 0.63 and satisfies the site symmetry requirement by assuming two, equally populated, centrosymmetrically disposed orientations. As a result of these two orientations the $[Mo_2S_7]^{2-}$ component appears as the hypothetical anti isomer of the $[Mo_2S_8]^{2-}$ thio anion (Figure 3). The *anti*-$[Mo_2S_4]^{2+}$ core has been found previously in the structure of the *anti*-$[Mo_2S_4(S_2C_2H_4)_2]^{2-}$ complex.[22] In fact both the 0.37/0.63 $[Mo_2S_6]^{2-}/[Mo_2S_7]^{2-}$ and the 0.685/0.315 $[Mo_2S_6]^{2-}$/*anti*-$[Mo_2S_8]^{2-}$ combinations give the same $Mo_2S_{6.63}$ stoichiometry and are crystallographically indistinguishable structure refinement models. The 0.37/0.63 $[Mo_2S_6]^{2-}/[Mo_2S_7]^{2-}$ combination was chosen as the chemically correct one and was verified by the independent synthesis, structural characterization, and spectroscopic characteristics of the 100% pure $[Ph_4P]_2[Mo_2S_6]$ and $[Ph_4P]_2[Mo_2S_7]$ complexes. The structural details of II, III, and IV are shown in Table VII. As a result of the disorder in II, precise bond distances and angles for the two new thio anions are more reliably obtained from the structures of pure $[Ph_4P]_2[Mo_2S_6]$ and $[Ph_4P]_2[Mo_2S_7]$. A calculation of the Mo–Mo and the Mo–S(2) (disorder-affected) distances by using the 0.37/0.63 $[Mo_2S_6]^{2-}/[Mo_2S_7]^{2-}$ model and the corresponding distances obtained from the structures of III and IV gave values of 2.852 (6) and 2.143 (3) Å and was in good agreement with the crystallographically determined values in II of 2.846 (1) and 2.126 (2) Å.

The $[Mo_2S_6]^{2-}$ anion consists of two tetrahedral Mo^VS_4 units sharing an edge and represents the simplest Mo thio anion known other than MoS_4^{2-}. The mean S–Mo–S angle of 109.4°[14] (range 103.2 (1)–113.3 (1)°) indicates slightly distorted tetrahedral geometry for each of the Mo atoms in III. The mean Mo–S bond length of 2.225 (1) Å is significantly longer than the mean Mo–S bond in the MoS_4^{2-} anion (2.177 (6) Å). The $[Mo_2S_7]^{2-}$ anion can be envisioned as either a structural derivative of $[Mo_2S_6]^{2-}$ where one of the terminal S^{2-} ligands has been replaced by a S_2^{2-} ligand or a structural derivative of $[(S_2)MoS(\mu\text{-}S)]_2^{2-}$ where a S_2^{2-} has been replaced by a S^{2-}.

The $[Mo^V{}_2S_2]^{6+}$ rhombic units in III and IV are very similar to other such units present in various dimeric Mo(V) sulfur complexes such as $[(S_2)MoS(\mu\text{-}S)]_2^{2-}$,[3b,c] $[(S_4)MoS(\mu\text{-}S)]_2^{2-}$,[3a] $[(S_4)MoS(\mu\text{-}S)_2SMo(S_2)]^{2-}$,[3a,d] $[(CS_4)MoS(\mu\text{-}S)]_2^{2-}$,[23] and others. The mean values of the Mo–S bridge bonds in I, III, and IV at 2.304 (5), 2.300 (1), and 2.303 (4) Å are almost identical and are very similar to the corresponding values in the $[(S_2)MoS(\mu\text{-}S)]_2^{2-}$[3b,c] and $[(CS_4)MoS(\mu\text{-}S)]_2^{2-}$[23] anions at 2.310 (2) and 2.315 (6) Å, respectively. This similarity is not unexpected since the *formal* oxidation states of the Mo atoms in all these dimers are the same. The complete delocalization of charge expected for the symmetric dimers is evident in the limited "spread" of the individual Mo–S bond lengths around the mean. In contrast asymmetric dimers such as I and IV show a considerably larger deviation from the mean that results from systematic differences between the Mo–S bridge bonds. In both I and IV the four-coordinate molybdenum atoms (Mo(2)) form the shorter Mo–S bridge bonds and have values for the mean Mo(2)–S bonds that are significantly shorter than those of the five-coordinate molybdenum atoms (Mo(1)). It is apparent that in I and IV the charge is partially localized on Mo(1), which is slightly reduced by comparison to Mo(2), which appears slightly oxidized.

Binary Molybdenum Sulfides. A great variety of binary Mo/S complexes are formed and can be isolated in reactions of the tetrathiomolybdate anion with various sulfide and polysulfide anions. The nature of the anionic products that can be isolated from these reactions depends to various extents upon (a) the amount of excess sulfur used (and the type of S_x^{2-} ligands present in the reaction mixtures), (b) the type of counterion used in the isolation of the complex anions, and (c) the type of solvent employed in the synthetic procedure.

In a previous report[3a] we attempted to interrelate the $[Mo_n(S_x)_y]^{2-}$ anions according to a general scheme taking into account known, structurally characterized, Mo/S complexes such as $[(S_4)_2MoS]^{2-}$,[3a] $[(S_2)MoS(\mu\text{-}S)]_2^{2-}$,[3b,c] $[(S_4)MoS(\mu\text{-}S)]_2^{2-}$,[3a] $[(S_4)MoS(\mu\text{-}S)_2SMo(S)_2]^{2-}$,[3a,d] $[MoS(MoS_4)_2]^{2-}$,[3e] and $[(S_2)_2Mo(\mu\text{-}S_2)]_2^{2-}$.[2a]

In this scheme, equilibria were proposed between the various Mo/S complex anions in reactions where gain or loss of elemental sulfur or sulfide ligands was taking place. An additional feature in this scheme was the inclusion of internal electron transfer in the structural transformation of some of these complex anions where oxidation or reduction of the molybdenum ions were affected by the breaking or making of S–S bonds (eq 3).

$$[S_x\text{–}S_x]^{2-} \underset{-2e^-}{\overset{2e^-}{\rightleftharpoons}} 2S_x^{2-} \qquad (3)$$

The synthesis and structural characterization of the new Mo/S anions $[MoS(MoS_4)(S_4)]^{2-}$, $[Mo_2S_7]^{2-}$, and $[Mo_2S_6]^{2-}$ completes the $[Mo_2S_n]^{2-}$ series (n = 6–12). The reactivity characteristics of the new anions, reported herein, are consistent with the scheme proposed earlier and reveal a rational approach for the synthesis of the homologous $[Mo_2(S)_n(S_2)_{6-n}]^{2-}$ anions. In this approach (Figure 6) any of the six homologues hypothetically could be obtained from any other by either the addition of sulfur or the abstraction of sulfur by triphenylphosphine.

---

(17) Kanatzidis, M. G.; Coucouvanis, D. *Acta Crystallogr., Sect. C: Cryst. Struct. Commun.* **1983**, *C39*, 835.

(18) Coucouvanis, D.; Stremple, P.; Simhon, E. D.; Swenson, D.; Baenziger, N. C.; Draganjac, M.; Chan, L. T.; Simopoulos, A.; Papaefthymiou, V.; Kostikas, A.; Petrouleas, V. *Inorg. Chem.* **1983**, *22*, 293–308.

(19) Coucouvanis, D.; Baenziger, N. C.; Simhom, E. D.; Stremple, P.; Swenson, D.; Kostikas, A.; Simopoulos, A.; Petrouleas, V.; Papaefthymiou, V. *J. Am. Chem. Soc.* **1980**, *102*, 1730.

(20) Coucouvanis, D.; Simhom, E. D.; Stremple, P.; Ryan, M.; Swenson, D.; Baenziger, N. C.; Simopoulos, A.; Papaefthymiou, V.; Kostikas, A.; Petrouleas, V. *Inorg. Chem.* **1984**, *23*, 741–749.

(21) Coucouvanis, D.; Hadjikyriacou, A.; Draganjac, M.; Kanatzidis, M. G.; Ileperuma, P. *Polyhedron* **1986**, *5*, 349.

(22) Bunzey, G.; Enemark, J. H.; Howie, J. K.; Sawyer, D. T. *J. Am. Chem. Soc.* **1977**, *99*, 4168.

(23) Coucouvanis, D.; Draganjac, M. *J. Am. Chem. Soc.* **1982**, *104*, 6820.

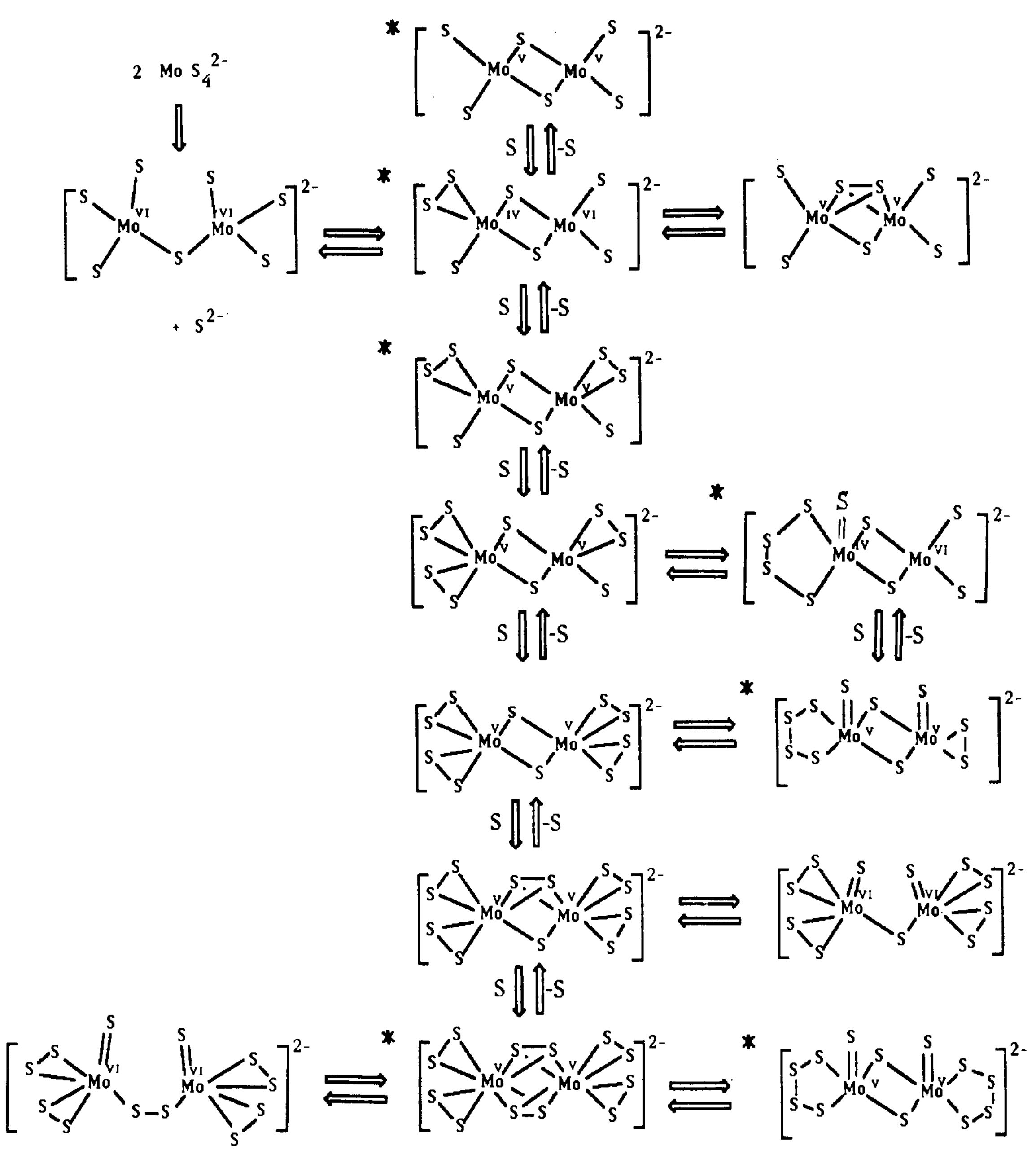

Figure 6. $[Mo_2(S)_n(S_2)_{6-n}]^{2-}$ anions: plausible isomers and their interconversions. The starred entries have been characterized structurally (see text for references).

Experimentally, this approach has been proven successful for the synthesis of most of the $[Mo_2(S)_n(S_2)_{6-n}]^{2-}$ complexes (or at times their internal-redox isomers) from any other member of the series, by stoichiometric reactions with BzSSSBz or Ph_3P.[24]

An examination of the entries in Figure 6 show that of the $[Mo_2(S)_n(S_2)_{6-n}]^{2-}$ anions, those with $n = 4$–6 have been characterized structurally. The anions with $n = 2$ and 3 have been structurally characterized as the "internal-redox" isomers $[(S_4)Mo(S)(\mu\text{-}S)_2(S)Mo(S_2)]^{2-}$ and $[MoS(MoS_4)(S_4)]^{2-}$, respectively. The anion with $n = 0$ has been isolated and structurally characterized as both the $[Mo_2(S_2)_6]^{2-}$ isomer and the $[(S_4)Mo(S)(\mu\text{-}S)_2(S)Mo(S_4)]^{2-}$ isomer. Finally the anion with $n = 1$ has not been isolated in any form. At this stage one could speculate that serendipitous, subtle changes in the synthetic procedures eventually may result in the stabilization and allow for the successful isolation of $[Mo_2(S)(S_2)_5]^{2-}$, $[Mo_2(S)_2(S_2)_4]^{2-}$, $[Mo_2(S)_3(S_2)_3]^{2-}$ and other Mo/S complexes (Figure 6) that, thus far, have been elusive to synthesis. We will continue our studies of the $[Mo_2(S)_n(S_2)_{6-n}]^{2-}$ anions and the coordination chemistry of the $[Mo_2S_6]^{2-}$ anion.

Acknowledgment. The financial support of this project by the National Science Foundation (Grant CH-83-0389) is gratefully acknowledged.

Supplementary Material Available: Tables SI–SIV, listing thermal parameters and the derived hydrogen positions for I–IV (10 pages); tables of calculated and observed structure factors for I–IV (40 pages). Ordering information is given on any current masthead page.

---

(24) Hadjikyriacou, A.; Coucouvanis, D., submitted for publication in *Inorg. Synth.*

(25) Johnson, C. K. "ORTEP"; Report ORNL-3794; Oak Ridge National Laboratory: Oak Ridge, TN, 1965.